Hindawi
Journal of Applied Mathematics
Volume 2022, Article ID 1131831, 11 pages
https://doi.org/10.1155/2022/1131831

Research Article

Asumu Fractional Derivative Applied to Edge Detection on SARS-COV2 Images

Gustavo Asumu Mboro Nchama,[1] **Leandro Daniel Lau Alfonso**,[2] **Roberto Rodríguez Morales**,[2] **and Ezekiel Nnamere Aneke**[3]

[1]*Universidad Nacional de Guinea Ecuatorial (UNGE), Calle Hassan II, Malabo, Equatorial Guinea*
[2]*Instituto de Cibernética, Matemática y Física (ICIMAF), Calle 15, No. 551, E/C y D, Vedado, Habana 4 C-P 10400, Cuba*
[3]*Enugu State University of Science and Technology, Enugu, Nigeria*

Correspondence should be addressed to Gustavo Asumu Mboro Nchama; asumu@matcom.uh.cu

Received 6 June 2021; Revised 24 September 2021; Accepted 12 November 2021; Published 4 January 2022

Academic Editor: Tudor Barbu

Edge detection consists of a set of mathematical methods which identifies the points in a digital image where image brightness changes sharply. In the traditional edge detection methods such as the first-order derivative filters, it is easy to lose image information details and the second-order derivative filters are more sensitive to noise. To overcome these problems, the methods based on the fractional differential-order filters have been proposed in the literature. This paper presents the construction and implementation of the Prewitt fractional differential filter in the Asumu definition sense for SARS-COV2 image edge detection. The experiments show that these filters can avoid noise and detect rich edge details. The experimental comparison show that the proposed method outperforms some edge detection methods. In the next paper, we are planning to improve and combine the proposed filters with artificial intelligence algorithm in order to program a training system for SARS-COV2 image classification with the aim of having a supplemental medical diagnostic.

1. Introduction

Digital image processing is an open field of research. The constant progress in this area has not been by itself, but in conjunction with other areas with which it is related such as mathematics, computing, and the increasing knowledge of certain organs of the human body that intervene in perception and in image manipulation. In addition to this, the development of hardware languages and programming languages, it became possible to use and apply mathematical methods in this area in a wide range of applications such as medicine, biology, archeology, geology, and astronomy. In the area of image processing, the edges of a digital image can be defined as transitions between two regions of significantly different gray levels. Edge detection in an image is extremely important and useful, as they provide valuable information about the boundaries of objects and facilitate many tasks, such as object recognition, and region segmentation, for which a variety of mathematical edge detection algorithms have been developed. The first class of algorithms used for such purposes are differential algorithms of first order. For example, in [1], the authors used the edge detection method to remove speckle sound and preserve diagnostic information without losing critical data in the image. In [2], the Canny and Sobel algorithms are used. The purpose of this study is to find the edges of the fracture and finally compare the two methods to find the best algorithm to do this. In [3], the Sobel edge detection algorithm is used previously to process the image, the edge image is acquired, the radar remote sensing image is analyzed from different angles, and then, the different radar remote sensing images are transformed. In [4], the authors applied the Roberts edge detector on gray and color images. The great inconvenience of this type of technique is that it produces thicker edges in images, and therefore, it has poor detection quality.

To mitigate this deficiency, other methods involving second-order differential operators have been proposed. Although thick edges can be avoided, they are extremely noise-sensitive methods. To detect edges in images while avoiding the abovementioned deficiencies, there have been proposed techniques involving fractional-order differential operators. For example, in [5], the genetic algorithm was used to get the optimal threshold levels for each image to enhance the edge detection of the fractional masks. In the paper [6], the fractional difference equation was obtained according to Grünwald-Letnikov fractional differential definition to construct some filter templates to extract the palm print image edge. The experiments showed that the fractional differential edge detection algorithm is better than integer-order differential methods. Based on these filters, experiment results showed that the algorithm can reduce noise and detect rich edge details than traditional methods. In [7], the authors proposed a short-edge detector algorithm without smoothing operation to deal with edge detection optimization. Experimentally, it has shown that in the proposed algorithm, the smoothing preprocess is no longer necessary due to the fact that the proposed fractional-order mask is expressed in terms of immunity to noise and the capability of detecting edges. Simulation results show how the quality of edge detection can be enhanced on adjusting the fractional-order parameter. In [8], the authors generalized the classical Sobel operator to constitute a fractional-order Sobel operator for edge detection. This operator was tested in brain MRI image segmentation. After making the comparison with the first-order Sobel operator, the experimental results showed that such kind of operators gives superior performance over conventional integer-order operators because they can detect more edge detail features of the medical images, as well as they are less sensitive to noise. In [9], the authors make a comparison between the integer and fraction edge detection and use one of the soft computing techniques which are fuzzy logic with integer and fraction edge detection. It shows that the soft computing technique for edge detection gives better results compared to the classical approach. In [10], the authors developed a new fractional-order edge detector via the Caputo-Fabrizio derivative. Using visual perception and statistical analysis, the proposed novel fractional mask without a singular kernel showed significant advantages over other compared methods. In [11], the authors aimed to extend the use of the Atangana-Baleanu fractional integral in edge detection. The performance of these methods was illustrated by several numerical simulations on natural images. In [12], the authors demonstrated how using an edge detector based on fractional-order differentiation can improve the criterion of thin detection, or detection selectivity in the case of parabolic luminance transitions, and the criterion of immunity to noise, which can be interpreted in terms of robustness to noise in general. In work [13], a study of the edge detection method based on the fractional derivative and Canny filter to determine information contained on the edges of digital images was carried out. In [14], the authors constructed fractional differential filters based on Grünwald-Letnikov definition to apply them in medical images. The proposed method showed superiority in comparison with Sobel and Prewitt filters. In [15], the authors discussed the capabilities of the fractional differential approach for the detection of textural features in two-dimensional digital images. In [16], a new way of constructing a fractional-based convolution mask with an application to image edge analysis was presented. The experiments conducted on the mask were done using some selected well-known synthetic, and medical images with realistic geometry demonstrated significant advantages over the other known methods. In the paper [17], a 2D-fractional differentiation mask was proposed to detect edge and features on natural images. The coefficients of the proposed mask were computed in a way that image details are detected and preserved. Experiments on texture images demonstrated the efficiency of the proposed filter compared to some existing techniques. In [18], the authors proposed a fractional-order-based edge detection technique for contrast enhancement of grayscale images, demonstrating the capability of varying the fractional differential order to analyze image feature and contrast using various performance metrics. In work [10], the Caputo-Fabrizio fractional-order derivative to generalize the first-order Sobel operator was considered. The resulting fractional mask was used to carry out edge analysis of medical images. The implementation of this method allowed to enhance the study of diseases such as breast cancer and breast calcifications. In [19], the authors presented a highly selective and noise-robust edge-relevant structure feature detection approach based on the fractional-order Gaussian derivatives by using the definition of the Caputo-Fabrizio derivative. Theoretical analysis and experimental results showed that the proposed method is capable of extracting complex edge-relevant structure features in natural images. In [20], a novel lossless image encryption algorithm based on edge detection and generalized chaotic maps for key generation was presented. The proposed system integrates different edge detectors, as well as various logistic maps for key generation. A comparison between the proposed scheme with existing cryptosystems showed that the proposed algorithm has higher statistical and cryptanalytic properties. In [21], the authors proposed the construction of Prewitt fractional-order filters in the Caputo and Caputo-Fabrizio senses to avoid thicker edges and the presence of noise when detecting edges in natural images. The experimental analysis proved that the proposed methods can suppress efficiently undesirable effects caused by traditional techniques. In [22], two novel central fractional-order masks were proposed to evaluate upon applying salt and pepper noise and Gaussian noise. The fractional-order parameter gives an extra degree of freedom in designing different masks. Numerical results proved that the proposed masks outperform the integer-order masks regarding both types of noise.

Even though the above outlined fractional differential-order models are able to avoid discontinuous edges, they keep producing thick edges. To avoid this fact and obtain thin edges, the authors propose a new way of construction of a fractional differential mask based on Asumu fractional-order definition for detecting edges in images with SARS-

COV2. This paper is structured as follows: Section 2 describes some well-known edge methods. Section 3 is a brief introduction to Asumu fractional differential definition. The proposed filter is constructed in Section 4. Section 5 describes the experimental results of the proposed algorithm, and Section 6 is related to the conclusions and future work.

2. Some of the Well-Known Differential Edge Methods

As we have said above, image edge detection methods have been developed and applied in different kinds of images in the last decade. The most efficient algorithms proposed are based on fractional differential-order operators. For example, in [21], the authors proposed the following filters:

$$\begin{bmatrix} \frac{2^{1-\alpha}-2\cdot 1^{1-\alpha}}{\Gamma(2-\alpha)} & \frac{2^{1-\alpha}-1^{1-\alpha}}{\Gamma(2-\alpha)} & \frac{1^{1-\alpha}}{\Gamma(2-\alpha)} \\ \frac{2^{1-\alpha}-2\cdot 1^{1-\alpha}}{\Gamma(2-\alpha)} & \frac{2^{1-\alpha}-1^{1-\alpha}}{\Gamma(2-\alpha)} & \frac{1^{1-\alpha}}{\Gamma(2-\alpha)} \\ \frac{2^{1-\alpha}-2\cdot 1^{1-\alpha}}{\Gamma(2-\alpha)} & \frac{2^{1-\alpha}-1^{1-\alpha}}{\Gamma(2-\alpha)} & \frac{1^{1-\alpha}}{\Gamma(2-\alpha)} \end{bmatrix}, \quad \begin{bmatrix} \frac{2^{1-\alpha}-2\cdot 1^{1-\alpha}}{\Gamma(2-\alpha)} & \frac{2^{1-\alpha}-2\cdot 1^{1-\alpha}}{\Gamma(2-\alpha)} & \frac{2^{1-\alpha}-2\cdot 1^{1-\alpha}}{\Gamma(2-\alpha)} \\ \frac{2^{1-\alpha}-1^{1-\alpha}}{\Gamma(2-\alpha)} & \frac{2^{1-\alpha}-1^{1-\alpha}}{\Gamma(2-\alpha)} & \frac{2^{1-\alpha}-1^{1-\alpha}}{\Gamma(2-\alpha)} \\ \frac{1^{1-\alpha}}{\Gamma(2-\alpha)} & \frac{1^{1-\alpha}}{\Gamma(2-\alpha)} & \frac{1^{1-\alpha}}{\Gamma(2-\alpha)} \end{bmatrix}, \tag{1}$$

making use of Caputo fractional differential $\alpha \in (0,1)$ order derivative. In work [5], the authors used an optimization technique to select the best threshold levels to enhance the edge detection algorithms based on the following fractional masks for $\alpha \in (0,1)$:

$$\begin{bmatrix} \frac{\alpha^2-\alpha}{6} & \frac{\alpha^2-\alpha}{6} & \frac{\alpha^2-\alpha}{6} \\ \frac{-\alpha}{5} & \frac{-\alpha}{5} & \frac{-\alpha}{5} \\ \frac{-\alpha}{5} & 1 & \frac{-\alpha}{5} \end{bmatrix}, \quad \begin{bmatrix} \frac{\alpha^2-\alpha}{6} & \frac{-\alpha}{5} & \frac{-\alpha}{5} \\ \frac{\alpha^2-\alpha}{6} & \frac{-\alpha}{5} & 1 \\ \frac{\alpha^2-\alpha}{6} & \frac{-\alpha}{5} & \frac{-\alpha}{5} \end{bmatrix}. \tag{2}$$

While in [21], a new way of construction of fractional differential filters in terms of the Caputo-Fabrizio derivative for $\alpha \in (0,1)$ was proposed:

$$\begin{bmatrix} \frac{2e^{-(a/(1-\alpha))}-e^{-2(a/(1-\alpha))}-1}{\alpha} & \frac{e^{-(a/(1-\alpha))}-e^{-2(a/(1-\alpha))}}{\alpha} & \frac{1-e^{-(a/(1-\alpha))}}{\alpha} \\ \frac{2e^{-(a/(1-\alpha))}-e^{-2(a/(1-\alpha))}-1}{\alpha} & \frac{e^{-(a/(1-\alpha))}-e^{-2(a/(1-\alpha))}}{\alpha} & \frac{1-e^{-(a/(1-\alpha))}}{\alpha} \\ \frac{2e^{-(a/(1-\alpha))}-e^{-2(a/(1-\alpha))}-1}{\alpha} & \frac{e^{-(a/(1-\alpha))}-e^{-2(a/(1-\alpha))}}{\alpha} & \frac{1-e^{-(a/(1-\alpha))}}{\alpha} \end{bmatrix}, \quad \begin{bmatrix} \frac{2e^{-(a/(1-\alpha))}-e^{-2(a/(1-\alpha))}-1}{\alpha} & \frac{2e^{-(a/(1-\alpha))}-e^{-2(a/(1-\alpha))}-1}{\alpha} & \frac{2e^{-(a/(1-\alpha))}-e^{-2(a/(1-\alpha))}-1}{\alpha} \\ \frac{e^{-(a/(1-\alpha))}-e^{-2(a/(1-\alpha))}}{\alpha} & \frac{e^{-(a/(1-\alpha))}-e^{-2(a/(1-\alpha))}}{\alpha} & \frac{e^{-(a/(1-\alpha))}-e^{-2(a/(1-\alpha))}}{\alpha} \\ \frac{1-e^{-(a/(1-\alpha))}}{\alpha} & \frac{1-e^{-(a/(1-\alpha))}}{\alpha} & \frac{1-e^{-(a/(1-\alpha))}}{\alpha} \end{bmatrix}. \tag{3}$$

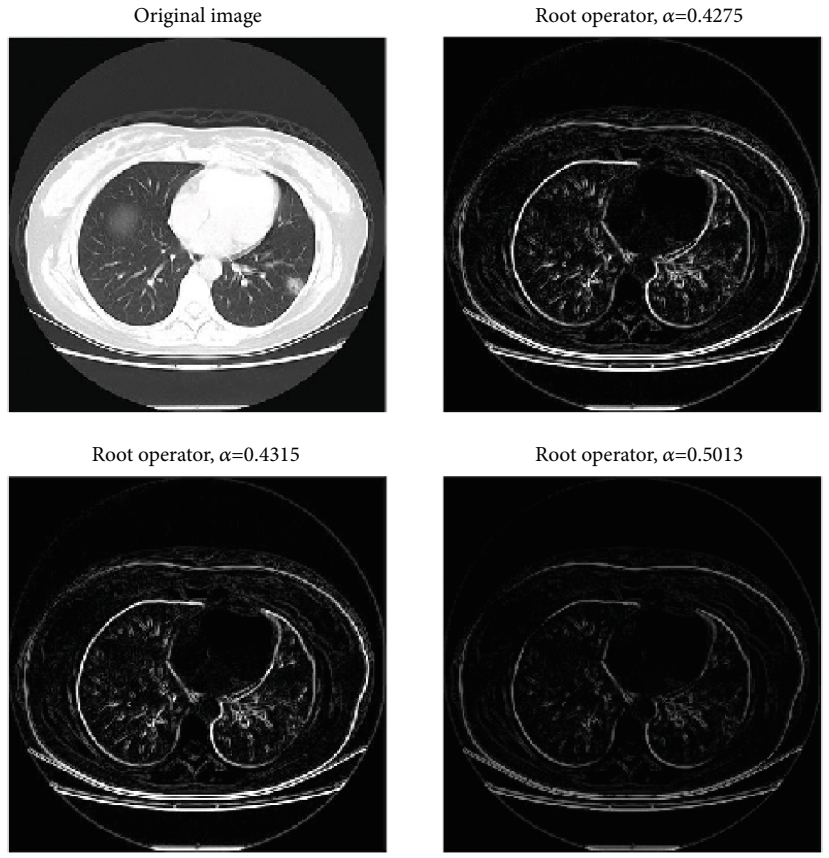

Figure 1: Image of the patient with COVID for three different values of α in the proposed model, root operator. The name of this image in the database is PIIS0140673620303603%8.png.

3. The Asumu Fractional Derivative Definition

In [23], Nchama suggested new fractional derivatives to improve theoretically the Riemann-Liouville and Caputo fractional derivatives. One of the derivatives is based upon the Riemann-Liouville view point and the other one on the Caputo approach. The Asumu fractional-order operator in the Caputo sense is defined as follows:

Definition 1. Let $a, b \in \mathbb{R}$, $a < b$, $n-1 < \alpha \leq n \in \mathbb{N}$, $f \in AC^n[a, b]$. The new fractional derivative in the Caputo sense of order α is defined by

$$ {}^{AC}D_{at}^{\alpha,n}(u(t)) \coloneqq \frac{1}{\Gamma(n-\alpha)} \cdot \frac{d^n}{dt^n}\left(\int_a^t (t-s)^{n+\alpha-1} \cdot \frac{d^n}{ds^n}u(s)ds\right), \tag{4} $$

where d^n/dt^n represents the ordinary derivative of order n with respect to the variable t.

In [23], we can find also the Laplace transform formula of equation (4) given by the following theorem:

Theorem 2. *Let $n-1 < \alpha \leq n \in \mathbb{N}$. Then,*

$$ \begin{aligned} \mathfrak{L}\left\{{}^{AC}D_{0t}^{\alpha,n}u(t)\right\} &= \frac{\Gamma(\alpha)}{\Gamma(n-\alpha)} \cdot \left[\prod_{k=1}^{n}(n+\alpha-k)\right] \cdot s^{-\alpha} \\ &\cdot \left\{s^n \mathfrak{L}\{u(t)\} - \sum_{k=0}^{n-1} s^{n-1-k}u^{(k)}(0)\right\}. \end{aligned} \tag{5} $$

Formula (4) can be rewritten in another way by making use of the following result:

Theorem 3. *Let $a \in \mathbb{R}$, $n-1 < \alpha \leq n \in \mathbb{N}$. Then,*

$$ \begin{aligned} {}^{AC}D_{at}^{\alpha,n}u(t) &= \frac{1}{\Gamma(n-\alpha)}\left[\prod_{k=1}^{n}(n+\alpha-k)\right] \\ &\cdot \int_a^t (t-s)^{\alpha-1}u^{(n)}(s)ds. \end{aligned} \tag{6} $$

Proof 4. Performing repeatedly the differentiation n times, we obtain

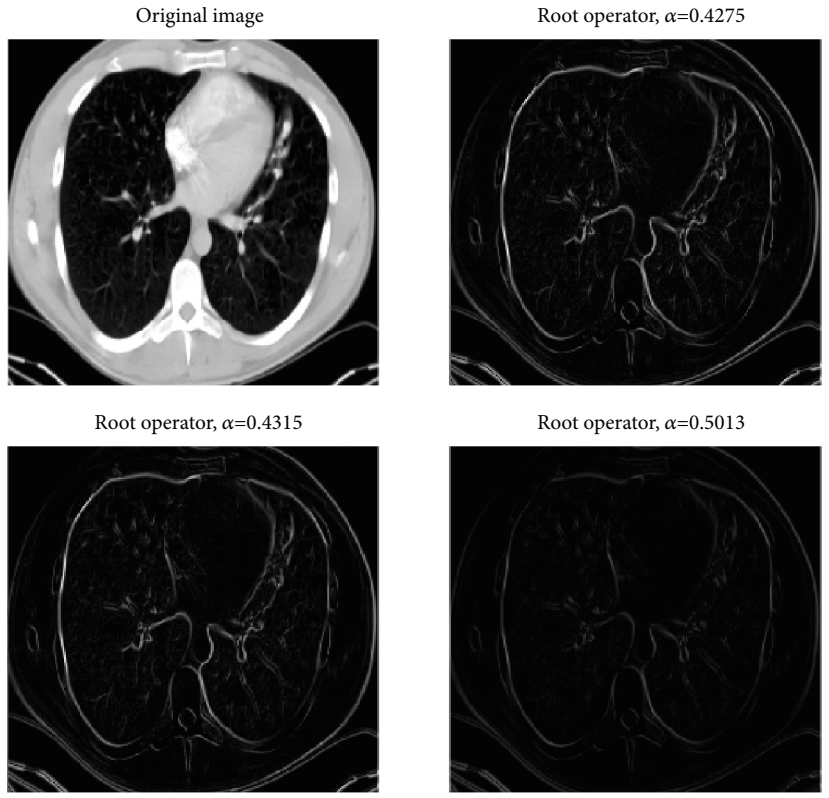

Figure 2: Image of the patient without COVID for three different values of α in the proposed model, root operator. The name of this image in the database is 957.png.

$$\frac{d^n}{dt^n}\int_a^t (t-s)^{n+\alpha-1}u^{(n)}(s)ds = \left[\prod_{k=1}^{n}(n+\alpha-k)\right] \cdot \int_a^t (t-s)^{\alpha-1}u^{(n)}(s)ds. \tag{7}$$

Multiplying both sides of (7) by $1/\Gamma(n-\alpha)$, we get (6). □

For $n = 1$, $0 < \alpha < 1$, the numerical approximation of formula (6) takes the form

$$\begin{aligned} {}^{AC}D_{0,x}^{\alpha,1}u(x) &= \frac{1}{\Gamma(1-\alpha)} \cdot \alpha \cdot \int_0^x (x-s)^{\alpha-1} \cdot u'(s)ds \\ &\approx \frac{\alpha}{\Gamma(1-\alpha)} \cdot \sum_{k=0}^{N-1} \int_{k\cdot x/N}^{(k+1)\cdot x/N} (x-\xi)^{\alpha-1} \cdot u'(\xi_k)d\xi. \end{aligned} \tag{8}$$

4. Asumu Fractional Differential-Order Filter

An image can be defined as a function of two variables. By approximating the function $u(x)$, we obtain the kernels which can be applied separately to the input image to produce separate measurements of the gradient component in each orientation (call these u_x and u_y). They can then be combined together to find the absolute magnitude of the gradient at each point and the orientation of that gradient. The gradient magnitude, in its square root way, is given by

$$|u| = \sqrt{(u_x)^2 + (u_y)^2}. \tag{9}$$

The derivative of a discrete function $u(x)$ is given by

$$\begin{aligned} \frac{du(x)}{dt} &= \lim_{h\longrightarrow 0} \frac{u(x+1)-u(x-1)}{1} \approx u(\mathrm{x}+1) - u(x-1) \\ &= -1 \cdot u(x-1) + 0 \cdot u(x) + 1 \cdot u(x+1). \end{aligned} \tag{10}$$

If we denote the horizontal derivative filter as h_x and the vertical derivative filter as h_y, then, from equation (10), the derivative filters h_x and h_y are expressed in vector forms as

$$h_x = [-1 \quad 0 \quad 1], \qquad h_y = \begin{bmatrix} -1 \\ 0 \\ 1 \end{bmatrix}. \tag{11}$$

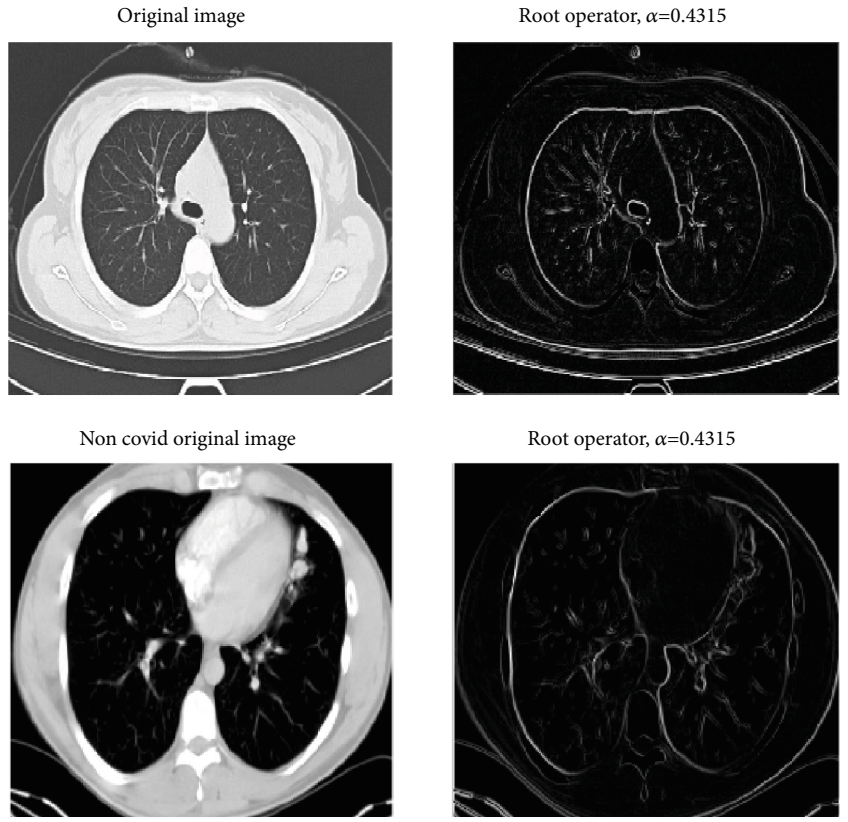

Figure 3: Images of patients with and without COVID for the same value of α in the proposed model, root operator. The name of the images in the first row is 2020.02.28.20029025-p23-182.png and corresponds to the patient with COVID, while the name of the images in the second row is 956.png and corresponds to the patient without COVID.

By approximating the function u with respect to the variable x using the forward finite difference scheme, we obtain

$$\begin{aligned}
&\int_{k\cdot x/N}^{(k+1)\cdot x/N} (x-\xi)^{\alpha-1}\cdot u'(\xi_k)d\xi \\
&\quad\approx u'(\xi_k)\cdot\int_{k\cdot x/N}^{(k+1)\cdot x/N}(x-\xi)^{\alpha-1}d\xi \\
&\quad\approx \frac{u((kx+x)/N)-u(kx/N)}{\Delta x}\cdot\int_{k\cdot x/N}^{(k+1)\cdot x/N}(x-\xi)^{\alpha-1}d\xi \\
&\quad= \frac{u((kx+x)/N)-u(kx/N)}{\Delta x}\cdot\frac{(x-\xi)^{\alpha}}{\alpha}\Bigg|_{k\cdot x/N}^{(k+1)\cdot x/N} \\
&\quad= \frac{u((kx+x)/N)-u(kx/N)}{\alpha\cdot\Delta x}\cdot\left[\left(x-\frac{(k+1)x}{N}\right)^{\alpha}-\left(x-\frac{kx}{N}\right)^{\alpha}\right] \\
&\quad= \frac{u((kx+x)/N)-u(kx/N)}{\alpha\cdot\Delta x}\cdot\left[\left(\frac{x\cdot N-(k+1)\cdot x}{N}\right)^{\alpha}-\left(\frac{N\cdot x-k\cdot x}{N}\right)^{\alpha}\right] \\
&\quad= \frac{u((kx+x)/N)-u(kx/N)}{\alpha\cdot\Delta x}\cdot\left[\left((N-(k+1))\cdot\frac{x}{N}\right)^{\alpha}-\left((N-k)\cdot\frac{x}{N}\right)^{\alpha}\right] \\
&\quad= \frac{u((kx+x)/N)-u(kx/N)}{\alpha\cdot\Delta x}\cdot[(N-k-1)^{\alpha}-(N-k)^{\alpha}]\cdot\left(\frac{x}{N}\right)^{\alpha}. \\
&\quad= \frac{u((kx+x)/N)-u(kx/N)}{\alpha\cdot(\Delta x)^{1-\alpha}}\cdot[(N-k-1)^{\alpha}-(N-k)^{\alpha}].
\end{aligned} \tag{12}$$

Then, replacing (12) into (8), we have

$$\begin{aligned}
{}^{AC}D_{0,x}^{\alpha,1}u(x,y) &\approx \frac{1}{\Gamma(1-\alpha)\cdot(\Delta x)^{1-\alpha}}\\
&\quad\cdot\sum_{k=0}^{N-1}\left[u\left(\frac{kx+x}{N},y\right)-u\left(\frac{kx}{N},y\right)\right]\\
&\quad\cdot[(N-k-1)^{\alpha}-(N-k)^{\alpha}]\\
&= \frac{1}{\Gamma(1-\alpha)\cdot(\Delta x)^{1-\alpha}}\cdot\{[N^{\alpha}-(N-1)^{\alpha}]u_0\\
&\quad+[2\cdot(N-1)^{\alpha}-(N-2)^{\alpha}-N^{\alpha}]u_1\\
&\quad+[2(N-2)^{\alpha}-(N-3)^{\alpha}-(N-1)^{\alpha}]u_2+\cdots\\
&\quad+[2(N-j)^{\alpha}-(N-j+1)^{\alpha}-(N-j-1)^{\alpha}]u_j\\
&\quad+(2^{\alpha}-1^{\alpha})u_{N-2}+(2\cdot1^{\alpha}-2^{\alpha})u_{N-1}-1^{\alpha}\cdot u_N\},
\end{aligned} \tag{13}$$

where the $N+1$ casual pixels $u_0, u_1, \cdots, u_N$ corresponding to $N+1$ nodes obtained after taking a partition of the interval $[0,x]$ in N equal parts with step $\Delta x = x/N$ are given by

$$\begin{cases}
u_0 = u(0),\\
u_1 = u(x/N),\\
\vdots\\
u_k = u(kx/N),\\
\vdots\\
u_N = u(x).
\end{cases} \tag{14}$$

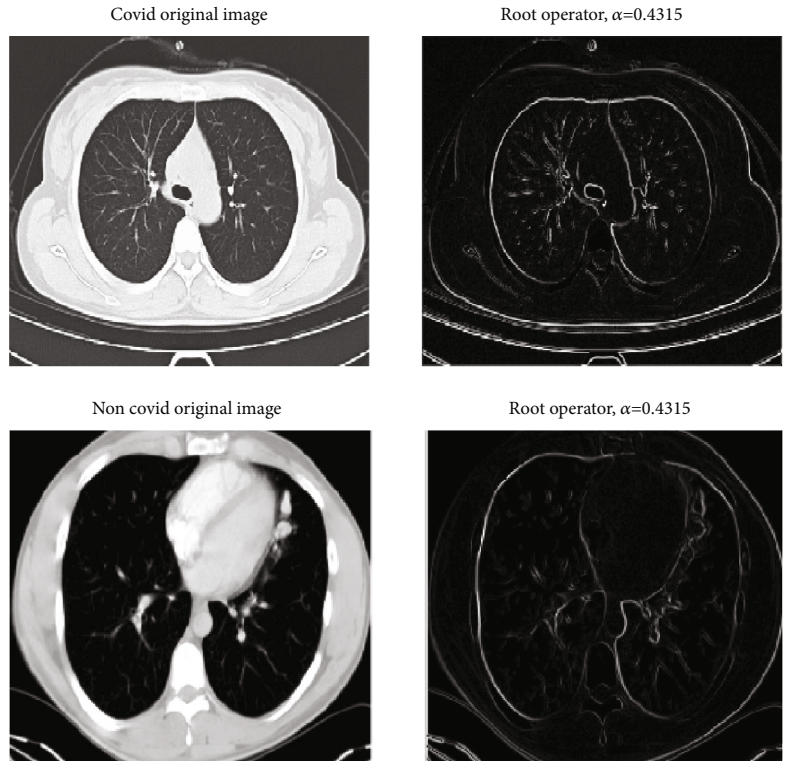

Figure 4: Images of patients with and without COVID for the same value of α in the proposed model, root operator. The name of the images in the first row is 2020.02.28.20029025-p23-182.png and corresponds to the patient with COVID, while the name of the images in the second row is 956.png and corresponds to the patient without COVID.

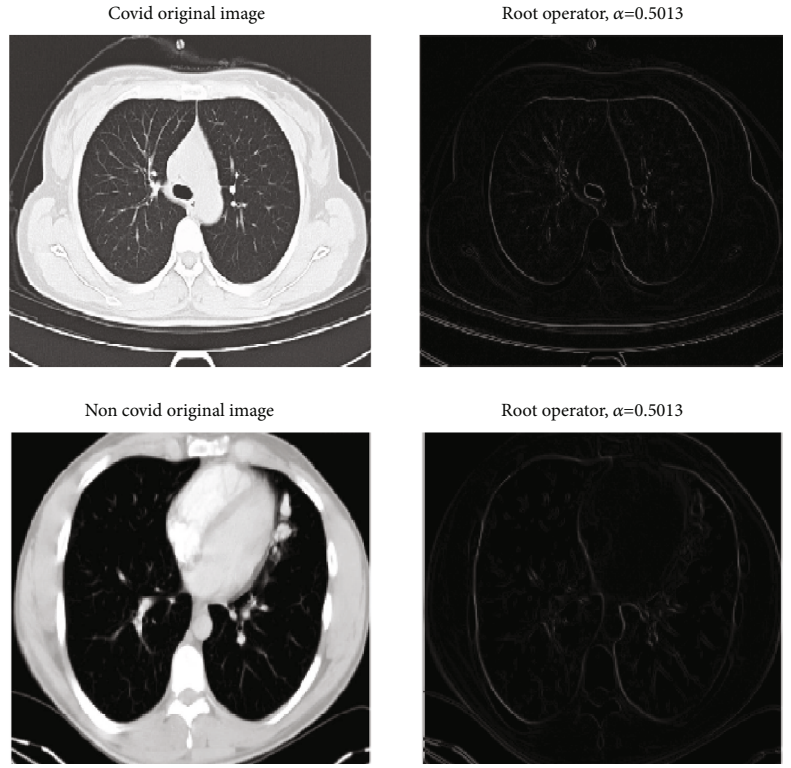

Figure 5: Images of patients with and without COVID for the same value of α in the proposed model, root operator. The name of the images in the first row is 2020.02.28.20029025-p23-182.png and corresponds to the patient with COVID, while the name of the images in the second row is 956.png and corresponds to the patient without COVID.

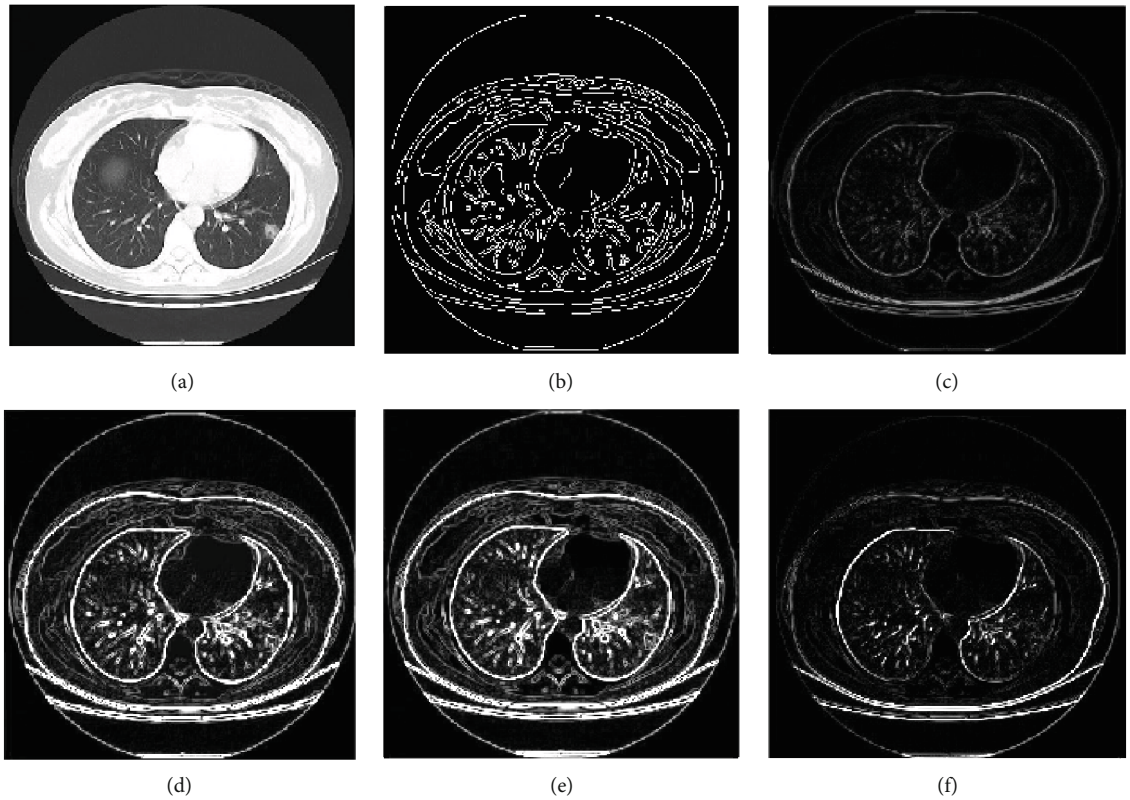

Figure 6: (a) Original image of the patient with COVID; (b) Canny method; (c) method proposed in [5]; (d, e) methods proposed in [21]; (f) our proposed method.

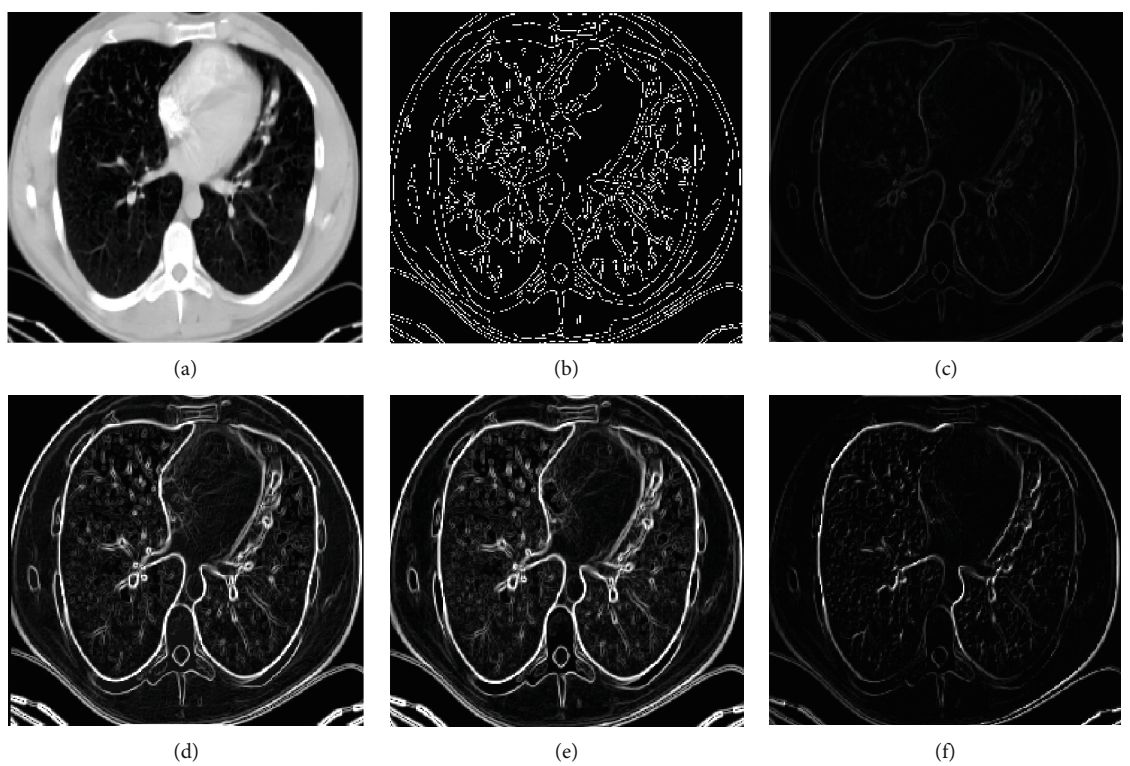

Figure 7: (a) Original image of the patient without COVID; (b) Canny method; (c) method proposed in [5]; (d, e) methods proposed in [21]; (f) our proposed method.

Analogously, with respect to variable y, we obtain

$$
\begin{aligned}
{}^{AC}D_{0,y}^{\alpha,1}u(x,y) \approx{}& \frac{1}{\Gamma(1-\alpha)\cdot(\Delta y)^{1-\alpha}} \\
&\cdot \sum_{k=0}^{N-1}\left[u\left(x,\frac{ky+y}{N}\right)-u\left(x,\frac{ky}{N}\right)\right] \\
&\cdot[(N-k-1)^{\alpha}-(N-k)^{\alpha}] \\
={}& \frac{1}{\Gamma(1-\alpha)\cdot(\Delta y)^{1-\alpha}}\cdot\{[N^{\alpha}-(N-1)^{\alpha}]u_0 \\
&+[2\cdot(N-1)^{\alpha}-(N-2)^{\alpha}-N^{\alpha}]u_1 \\
&+[2(N-2)^{\alpha}-(N-3)^{\alpha}-(N-1)^{\alpha}]u_2+\cdots \\
&+[2(N-j)^{\alpha}-(N-j+1)^{\alpha}-(N-j-1)^{\alpha}]u_j \\
&+(2^{\alpha}-1^{\alpha})u_{N-2}+(2\cdot 1^{\alpha}-2^{\alpha})u_{N-1}-1^{\alpha}\cdot u_N\}.
\end{aligned}
\tag{15}
$$

Since in a digital $2D$ gray image $u(x;y)$, the shortest distance on x and y coordinates is considered one pixel, then, we put $\Delta y = \Delta x = 1$. As a consequence, the approximate differences (13) and (15) can then be expressed in terms of the sum as

$$
{}^{AC}D_{0,x}^{\alpha,1}u(x,y) \approx \frac{1}{\Gamma(1-\alpha)}\cdot\sum_{k=0}^{N} c_{N-k}\cdot u_k \approx {}^{AC}D_{0,y}^{\alpha,1}u(x,y),
\tag{16}
$$

where the $N+1$ coefficients $\{c_k\}_{k=0,N}$ depending on parameter α are given as

$$
\begin{cases}
c_0 = \dfrac{(-1)^{\alpha}}{\Gamma(1-\alpha)}, \\
c_1 = \dfrac{2\cdot 1^{\alpha}-2^{\alpha}}{\Gamma(1-\alpha)}, \\
c_2 = \dfrac{2^{\alpha}-1^{\alpha}}{\Gamma(1-\alpha)}, \\
\vdots \\
c_j = \dfrac{2\cdot(N-j)^{\alpha}-(N-j+1)^{\alpha}-(N-j-1)^{\alpha}}{\Gamma(1-\alpha)}, \\
\vdots \\
c_{N-1} = \dfrac{2\cdot(N-1)^{\alpha}-(N-2)^{\alpha}-N^{\alpha}}{\Gamma(1-\alpha)}, \\
\vdots \\
c_N = \dfrac{N^{\alpha}-(N-1)^{\alpha}}{\Gamma(1-\alpha)}.
\end{cases}
\tag{17}
$$

Using expressions (13) and (15) for $N = 2$, we obtain

$$
\begin{aligned}
{}^{AC}D_{0x}^{\alpha,n}u(x,y) \approx{}& \frac{1}{\Gamma(1-\alpha)}\cdot\{(-1)^{\alpha}\cdot u(x,y)+(2\cdot 1^{\alpha}-2^{\alpha})\cdot u(x-1,y)\} \\
={}& \frac{2\cdot 1^{\alpha}-2^{\alpha}}{\Gamma(1-\alpha)}\cdot u(x-1,y)+\frac{(-1)^{\alpha}}{\Gamma(1-\alpha)}\cdot u(\mathrm{x},y) \\
&+0\cdot u(x+1,y),
\end{aligned}
\tag{18}
$$

$$
\begin{aligned}
{}^{AC}D_{0y}^{\alpha,n}u(x,y) \approx{}& \frac{1}{\Gamma(1-\alpha)}\cdot\{(-1)^{\alpha}\cdot u(x,y)+(2\cdot 1^{\alpha}-2^{\alpha})\cdot u(x,y-1)\} \\
={}& \frac{2\cdot 1^{\alpha}-2^{\alpha}}{\Gamma(1-\alpha)}\cdot u(x,y-1)+\frac{(-1)^{\alpha}}{\Gamma(1-\alpha)}\cdot u(x,y) \\
&+0\cdot u(x,y+1).
\end{aligned}
\tag{19}
$$

In relation to the vectors in (11), the right-hand side of (10) can be interpreted in the following way: the first, second, and third components of the vectors in (11) are considered as coefficients of $u(x-1)$, $u(x)$, and $u(x+1)$, respectively. Basing on this idea, we obtain from (18) (or from (19)) the following vectors:

$$
\begin{bmatrix}
\dfrac{2\cdot 1^{\alpha}-2^{\alpha}}{\Gamma(1-\alpha)} & \dfrac{(-1)^{\alpha}}{\Gamma(1-\alpha)} & 0
\end{bmatrix},
\quad
\begin{bmatrix}
\dfrac{2\cdot 1^{\alpha}-2^{\alpha}}{\Gamma(1-\alpha)} \\
\dfrac{(-1)^{\alpha}}{\Gamma(1-\alpha)} \\
0
\end{bmatrix}.
\tag{20}
$$

From (20), we obtain finally the following matrix:

$$
\begin{bmatrix}
\dfrac{2\cdot 1^{\alpha}-2^{\alpha}}{\Gamma(1-\alpha)} & \dfrac{(-1)^{\alpha}}{\Gamma(1-\alpha)} & 0 \\
\dfrac{2\cdot 1^{\alpha}-2^{\alpha}}{\Gamma(1-\alpha)} & \dfrac{(-1)^{\alpha}}{\Gamma(1-\alpha)} & 0 \\
\dfrac{2\cdot 1^{\alpha}-2^{\alpha}}{\Gamma(1-\alpha)} & \dfrac{(-1)^{\alpha}}{\Gamma(1-\alpha)} & 0
\end{bmatrix},
\tag{21}
$$

$$
\begin{bmatrix}
\dfrac{2\cdot 1^{\alpha}-2^{\alpha}}{\Gamma(1-\alpha)} & \dfrac{2\cdot 1^{\alpha}-2^{\alpha}}{\Gamma(1-\alpha)} & \dfrac{2\cdot 1^{\alpha}-2^{\alpha}}{\Gamma(1-\alpha)} \\
\dfrac{(-1)^{\alpha}}{\Gamma(1-\alpha)} & \dfrac{(-1)^{\alpha}}{\Gamma(1-\alpha)} & \dfrac{(-1)^{\alpha}}{\Gamma(1-\alpha)} \\
0 & 0 & 0
\end{bmatrix},
\tag{22}
$$

which are Prewitt fractional filters in the sense of Asumu derivative.

5. Experimental Results

In this section, we are going to illustrate the results obtained through the proposed edge detection filters. For the construction of filters (21) and (22), only the first two coefficients are considered in this paper and the two coefficients are $c_0 = (-1)^{\alpha}/\Gamma(1-\alpha)$ and $c_1 = (2 \cdot 1^{\alpha} - 2^{\alpha})/\Gamma(1-\alpha)$. Figures 1–5 show the edges as the results of applying the proposed method on SARS-COV2 and not SARS-COV2 images with different values of differential order. Based on the results shown in Figures 1–5, we can see that the proposed method can not only avoid thicker edges but also prevent noise when detecting edges. The proposed filters have demonstrated the capability of obtaining different edge detection images by varying the fractional differential order. After comparing the proposed method with others given in the literature (see Figures 6 and 7), we noted that our propose is to overcome them in some aspect: the proposed edge detector has the advantage that it can produce thinner edges than those obtained with the compared methods. However, techniques proposed in [21] produce more toned edges. In short, if the goal of a researcher is to obtain thinner edges, our propose becomes a firm candidate. But if the objective is to get edges with more tone, techniques like [21] are better. After using different values of fractional order α, we concluded that when α tends to be 0, images appear clearer. Otherwise, when we study the filters with α values close to 1, we see the opposite behavior. However, when applying the filter by using values of α on the interval [0.4, 0.51], we obtained images with better edges.

6. Conclusion and Future Scope

The goal of this paper has been to analyze the results by means of the proposed fractional differential-order edge detection filters. After doing the visual analysis of edge detection, we have observed that the proposed filters can control the degree of edge detection by varying the fractional differential order as well as it provides good localization and detects sharper edges. The experimental analysis of the proposed filters with different fractional-order α values showed that images corresponding with α values near 0 look clearer. While fractional α values close to 1 give darker images. The fractional order α values for better edge detection image belong to the interval [0.4, 0.51]. As a future work, we are planning to improve and combine these fractional filters with artificial intelligence algorithm in order to program a training system for SARS-COV2 image classification with the aim of having a supplemental medical diagnostic.

Data Availability

To support this study, the image database under the web direction http://medicalsegmentation.com/covid19/ was used.

Conflicts of Interest

The authors declare that they have no conflict of interest.

Acknowledgments

This work is supported by Universidad Nacional de Guinea Ecuatorial (UNGE) and Instituto de Cibernética, Matemática y Física (ICIMAF), under the auspices of the project: Programa Nacional de Nanociencia y Nanotecnología: Mejoramiento, segmentación y aprendizaje profundo de nanobioimágenes. Procesamiento paralelo de grandes volúmenes de datos.

References

[1] M. R. Kumar, J. L. Prasanna, V. S. H. Vardhan et al., "Image enhancement for ultrasound images using Sobel edge detection," *Journal of Critical Reviews*, vol. 7, no. 13, pp. 390–394, 2020.

[2] M. Shafiabadi, A. Kamkar-Rouhani, S. R. G. Riabi, A. R. Kahoo, and B. Tokhmechi, "Identification of reservoir fractures on FMI image logs using Canny and Sobel edge detection algorithms," *Oil & Gas Science and Technology-Revue dIFP Energies Nouvelles*, vol. 76, p. 10, 2021.

[3] G. Chen, Z. Jiang, and M. M. Kamruzzaman, "Radar remote sensing image retrieval algorithm based on improved Sobel operator," *Journal of Visual Communication and Image Representation*, vol. 71, article 102720, 2020.

[4] H. S. Prasantha, "Edge detection algorithms on digital signal processor DM642," *International Journal of Creative Research Thoughts*, vol. 8, no. 9, pp. 1–6, 2020.

[5] W. S. El Araby, A. H. Madian, M. A. Ashour, I. Farag, and M. Nassef, "Radiographic images fractional edge detection based on genetic algorithm," *Image*, vol. 11, no. 4, pp. 158–166, 2018.

[6] C. Chi and F. Gao, "Palm print edge extraction using fractional differential algorithm," *Journal of Applied Mathematics*, vol. 2014, Article ID 896938, 7 pages, 2014.

[7] M. Mekideche and Y. Ferdi, "Edge detection optimization using fractional order calculus," *The International Arab Journal of Information Technology (IAJIT)*, vol. 16, no. 5, pp. 827–832, 2019.

[8] D. Tian, D. Li, and Y. Zhang, "Medical image segmentation based on fractional-order derivative," in *2015 Asia-Pacific Energy Equipment Engineering Research Conference*, pp. 453–456, Atlantis Press, 2015.

[9] W. S. ElAraby, A. H. Median, M. A. Ashour, I. Farag, and M. Nassef, "Fractional Canny edge detection for biomedical applications," in *2016 28th International Conference on Microelectronics (ICM)*, pp. 265–268, Cairo, Egypt, December 2016.

[10] J. E. Lavín-Delgado, J. E. Solís-Pérez, J. F. Gómez-Aguilar, and R. F. Escobar-Jiménez, "A new fractional-order mask for image edge detection based on Caputo-Fabrizio fractional-order derivative without singular kernel," *Circuits, Systems, and Signal Processing*, vol. 39, no. 3, pp. 1419–1448, 2020.

[11] B. Ghanbari and A. Atangana, "Some new edge detecting techniques based on fractional derivatives with non-local and non-singular kernels," *Advances in Difference Equations*, vol. 2020, no. 1, 19 pages, 2020.

[12] B. Mathieu, P. Melchior, A. Oustaloup, and C. Ceyral, "Fractional differentiation for edge detection," *Signal Processing*, vol. 83, no. 11, pp. 2421–2432, 2003.

[13] N. Nema, P. Shukla, and V. Soni, "Fractional calculus based via edge appreciation act in digital image processing,"

International Research Journal of Modernization in Engineering Technology and Science, vol. 2, no. 4, pp. 1–7, 2020.

[14] R. John and N. Kunju, "Detection of Alzheimer's disease using fractional edge detection," *Journal of Biodiversity & Endangered Species*, vol. 9, no. 3, p. 2, 2018.

[15] P. U. Yi-Fei, "Fractional differential analysis for texture of digital image," *Journal of Algorithms & Computational Technology*, vol. 1, no. 3, pp. 357–380, 2007.

[16] P. Amoako-Yirenkyi, J. K. Appati, and I. K. Dontwi, "A new construction of a fractional derivative mask for image edge analysis based on Riemann-Liouville fractional derivative," *Advances in Difference Equations*, vol. 2016, no. 1, 23 pages, 2016.

[17] M. Hacini, A. Hacini, H. Akdag, and F. Hachouf, "A 2D-fractional derivative mask for image feature edge detection," in *3rd International Conference on Advanced Technologiesfor Signal and Image Processing - ATSIP'2017*, pp. 1–6, Fez, Marroco, 2017.

[18] A. Nandal, H. Gamboa-Rosales, A. Dhaka et al., "Image edge detection using fractional calculus with feature and contrast enhancement," *Circuits, Systems, and Signal Processing*, vol. 37, no. 9, pp. 3946–3972, 2018.

[19] G. Zhang, J. Liu, J. Wang et al., "FoGDbED: fractional-order Gaussian derivatives-based edge-relevant structure detection using Caputo-Fabrizio definition," *Digital Signal Processing*, vol. 98, article 102639, 2020.

[20] S. M. Ismail, L. A. Said, A. G. Radwan, A. H. Madian, and M. F. Abu-ElYazeed, "A novel image encryption system merging fractional-order edge detection and generalized chaotic maps," *Signal Processing*, vol. 167, article 107280, 2020.

[21] G. A. M. Nchama, L. D. L. Alfonso, and A. P. Cosme, "Natural images edge detection using Prewitt fractional differential algorithm via Caputo and Caputo-Fabrizio definitions," *Global Journal of Pure and Applied Mathematics*, vol. 16, no. 6, pp. 789–809, 2020.

[22] S. M. Ismail, L. A. Said, A. H. Madian, and A. G. Radwan, "Fractional-order edge detection masks for diabetic retinopathy diagnosis as a case study," *Computers*, vol. 10, no. 3, p. 30, 2021.

[23] G. A. M. Nchama, "New fractional derivatives in the sense of Riemann-Liouville and Caputo approaches," *New Trends in Mathematical Sciences*, vol. 4, no. 8, pp. 9–24, 2020.